Dependence of Material Properties on Processing History during Wire Drawing of Commercially Doped Tungsten Lamp Wire.

P. F. Browning, C. L. Briant, B. A. Knudsen
General Electric Corporate Research and Development
1 River Road
Schenectady, NY 12345

The dependence of the material properties of doped tungsten wire on processing history was investigated during the initial stages of wire drawing. Mechanical properties were found to be related to various sub-structural features, which in turn were found to be related to the various dynamic recovery mechanisms that can occur during deformation. The extent of dynamic recovery that took place at a given wire drawing pass was found to depend on the true strain content and deformation temperature. Because sub-structural development takes place throughout the wire drawing process, it was found that knowledge of the entire processing history of a specimen was required in order to predict its mechanical properties.

INTRODUCTION:

During the drawing of tungsten wire, breakage during processing and handling can cause significant material loss and reduce process efficiency. In many cases, breakage occurs as a result of the wire having insufficient ductility to withstand the coiling and handling processes required during wire drawing. To avoid this problem, we must understand the factors which affect ductility.

A single crystal of tungsten will exhibit substantial ductility at room temperature[1]. However, because the grain boundaries of tungsten are very weak in comparison to individual grains, fracture in annealed polycrystalline samples usually initiates at grain boundaries and crack propagation occurs in a highly intergranular fashion, resulting in brittle failure[2]. In 1912, Coolidge patented the process for manufacturing ductile tungsten[3]. It is now well understood that the dramatic ductility increase that Coolidge achieved from heavy mechanical deformation of tungsten can be attributed to the microstructure that was developed. During mechanical deformation, grains elongate into fibers. As this occurs, the number of transverse grain boundaries per unit length is reduced, which causes a higher fraction of an applied load to be carried by the fibers themselves. The result is that fracture begins to occur in a transgranular fashion, with increasing plastic deformation occurring in individual fibers[4]. By this mechanism the ductile-brittle transition temperature (DBTT) of tungsten decreases with increasing strain content[5]. With enough deformation, Coolidge found that tungsten can develop a DBTT well below room temperature[3].

In this paper we report a study of the evolution of material properties in tungsten during wire drawing. Particular attention will be paid to the effect of drawing temperature history on the room temperature ductility of the wire.

EXPERIMENTAL PROCEDURE

The starting material for this study was twenty rolled and swaged rods of General Electric grade 218 NS tungsten which had received a recrystallization anneal. This material was supplied by the Tungsten Products Plant of the General Electric Company.

Two draw benches were used for this work. For the first two drawing passes, a straight bench was used because the ductility of the wire was not sufficient to allow for coiling with available equipment. This bench was instrumented to measure drawing temperature, draw speed and draw force. The remaining five drawing passes were performed on a draw bench which had a four foot diameter take-up coil. The drawing force was supplied by the rotation of the take-up coil. This bench was instrumented to measure drawing temperature and drawing speed. In addition, the draw force was measured indirectly by monitoring the power output of the take-up coil motor. Back tension did not exceed five pounds on either draw bench. Die temperatures were 500 C $\pm$ 25 C. Commercially available suspensions of colloidal graphite in water were used as the wire drawing lubricants; their exact compositions are proprietary information of their manufacturers.

The starting material of 6.70 mm recrystallized rod was swaged in the laboratory using an experimental reduction schedule. Three swaging passes were performed, with each resulting in an area reduction of approximately 35%. Using this reduction schedule, the starting material was swaged to a final diameter of 3.40 mm. Two experimental temperature schedules, denoted H (for high temperature) and L (for low temperature), were studied. Ten rods were swaged using each temperature schedule. The pertinent processing parameters are listed below in table 1.

Table 1: Experimental Swaging Process Schedules

Swage Pass	Exit Diameter (mm)	Reduction in Area (Percent)	Schedule H Furnace Exit Temp (Celsius)	Schedule L Furnace Exit Temp (Celsius)	Die Exit Velocity (m/min)
1	5.26	34.29	1300	1150	2.13
2	4.27	34.13	1300	1150	2.13
3	3.40	36.38	1300	1150	2.13

Each lot of 10 swaged rods was then divided into 3 sub-lots of 3 to 4 rods each. Each of these sub-lots was drawn through seven passes using one of three temperature schedules. See Table 2 for a listing of the nominal drawing temperatures (and other processing variables) used for each schedule.

Table 2: Experimental Wire Drawing Process Schedules

Draw Pass	Exit Diam (mm)	Reduction in Area (Percent)	Schedule 1 Die Entry Temp (Celsius)	Schedule 2 Die Entry Temp (Celsius)	Schedule 3 Die Entry Temp (Celsius)	Draw Speed (m/min)
1	2.67	38.60	1050 *	1000	900	6.1
2	2.08	39.01	1050	1000	900	6.1
3	1.57	42.83	1000	950	825	7.6
4	1.19	42.53	975	900	800	7.6
5	0.94	38.03	975	900	800	7.6
6	0.76	34.26	900	825	725	9.1
7	0.64	30.56	875	825	725	9.1

* Temperatures measured at die entry. Actual value varied by ± 15 C from nominal.

Because we were interested in developing an understanding of the effect of drawing temperature history on wire properties, a method was required for quantifying the drawing temperature history of a sample. We chose to accomplish this by carefully selecting drawing temperature schedules such that drawing temperatures decreased in an approximately linear fashion with increasing true strain. The slope of this decrease was chosen to be approximately equal to that of a plot of DBTT as a function of true strain. Figure 1 shows a plot of the drawing temperature schedules listed above, as well as the DBTT of NS tungsten wire[5], plotted as a function of true strain. Because the linear slopes of the temperature schedules shown in figure one are equal and because the same reduction schedule was used throughout, it was possible to uniquely quantify a sample's thermomechanical processing history with a single temperature. We arbitrarily chose to use the average drawing

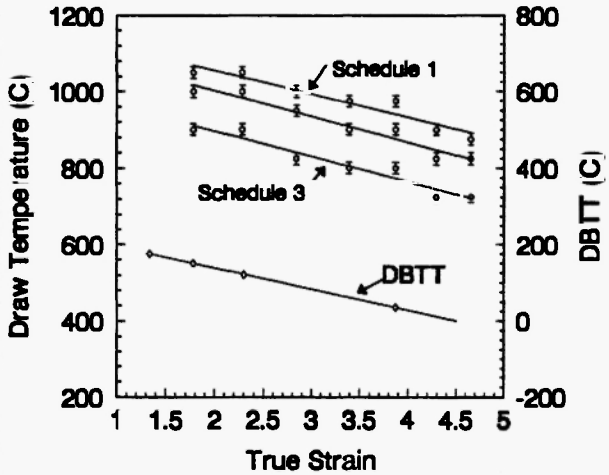

Figure 1: Nominal drawing temperature schedules and ductile/brittle transition temperature vs. true strain. DBTT data courtesy D.R. Hennessey[5]

temperature to characterize thermal drawing history. The difference between the average drawing temperatures of two experimental samples therefore is a characterization of the difference in drawing temperature history. It is important to note that this method will not be valid in the general case of comparing two drawing temperature schedules where temperature is decreased in a non-linear fashion with increasing true strain or when the slope of the decrease is not constant for all schedules.

The average drawing temperature was calculated using the following equation:

$$\text{Average Draw Temperature} = \sum_{i=1..n} T_i / n \qquad (1)$$

where T_i equals the draw temperature, measured at die entry, of the i^{th} drawing pass and n equals the total number of drawing passes (n = 1..7 in this study).

True strain is commonly used to quantify deformation[12] and will be used in this report. This quantity, which indicates the amount of uniform deformation that has been performed on a workpiece since the final recrystallization anneal, was determined using the following equation:

$$\varepsilon = 2 \ln(D_o/D) \qquad (2)$$

where ε equals true strain, D_o equals the rod diameter at the last recrystallization anneal and D equals the wire diameter of interest.

Two specimens were tested for room temperature (RT) tensile properties for each experimental sample at each drawing pass. Tensile elongation was used to quantify room temperature wire ductility. Total sample length was five inches and gauge length was one inch. Tests were carried out using a strain rate of 3.3×10^{-4} s^{-1}.

Electrical residual resistivity ratio measurement is a sensitive measure of the extent of dynamic recovery that has occurred during processing[6]. The residual resistivities of seven samples of 0.64 mm wire were measured. Sample length for this measurement was 30.5 cm and each sample was tested twice.

In addition to the work listed above, a separate set of drawing trials were performed to investigate the relationship between drawing stress and drawing temperature at each of the seven drawing passes listed in table 1.

For the first two draw passes, sample lengths were approximately eleven feet (due to limitations imposed by the length of the straight draw bench). A number of samples were drawn at various temperatures and the draw force was recorded for each of these samples. For the remaining five draw passes (for which the four foot take-up coil draw bench was used) longer lengths were possible. Drawing temperature was varied during the drawing of a single sample to obtain the draw force required (measured as coil motor power) for different drawing temperatures. The same equipment, procedures and starting materials that were discussed above were used in these experiments.

Two of the samples which were used in characterizing the relationship between draw stress and draw temperature at the 2.67 mm draw pass were taken from the same 3.40 mm swaged rod. One of these samples was drawn to 2.67 mm at 800 C, while the other was drawn at 1100 C. Transmission electron microscopy was used to evaluate substructural development in these samples.

RESULTS

The relationship between draw stress and draw temperature was less straight-forward than expected. It was found that two distinct slope changes occurred in a plot of draw stress vs. draw temperature. Figure 2a shows the nature of these slope changes for the draw pass from 2.67 mm to 2.08 mm diameter. Figures 2b and 2c show similar plots for the draw passes from 2.08 mm to 1.57 mm diameter and 1.57 mm to 1.19 mm diameter, respectively. Notice that the temperatures at which the slope changes occur are different for each of the drawing passes shown. For the first four draw passes, we were able to determine the temperature at which the lower temperature slope change occurred. This temperature is indicated by a vertical arrow in figures 2a - 2c. Although we saw evidence of the lower temperature slope change for wire sizes below 1.19 mm, the range of temperatures investigated did not allow for unambiguous determination of the temperature at which this slope change occurred (due in part to pyrometer limitations).

It was found that the draw stress vs. draw temperature plot retained

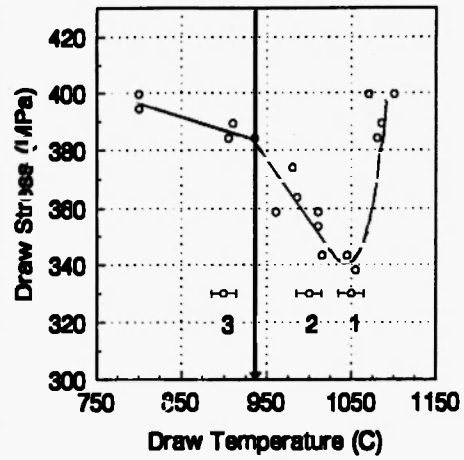

Figure 2a: Draw stress vs. draw temperature for 2.67 mm to 2.08 mm draw pass. There are slope changes at 940 C and 1070 C. The range of drawing temperatures used for each of the three drawing schedules investigated are shown and numbered.

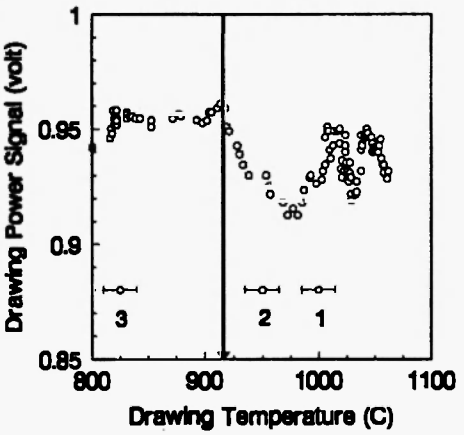

Figure 2b: Draw power vs. temperature for 2.08 to 1.57 mm draw pass. There are slope changes at 920 C and 975 C. The range of temperatures used in the three drawing schedules are shown and numbered.

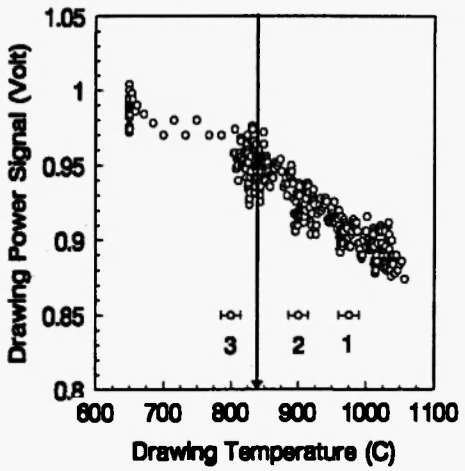

Figure 2c: Draw power vs. draw temperature for 1.57 mm to 1.19 mm draw pass. The lower temperature slope change occurs at 835 C. The high temperature slope change was not reached. The range of temperatures used for each schedule are shown and numbered.

these slope changes for drawing speeds ranging from 2 to 12 m/s. We also noticed that areas of the wire in which the lubricating layer was discontinuous were apparent at temperatures above the high temperature slope change and concluded that this slope change was due to thermal breakdown of the graphite lubricant through spallation and oxidation. The fact that lubricant breakdown did not occur at consistent temperatures in figures 2a - 2c may be related to poor control of furnace air/gas mixtures as we would expect that oxidation of the lubricant would be affected by the availability of free oxygen during combustion.

Room temperature (RT) tensile testing was performed on each wire sample at each drawing pass. Figure 3 shows a plot of the average percent elongation of all tensile samples vs. true drawing strain and indicates that

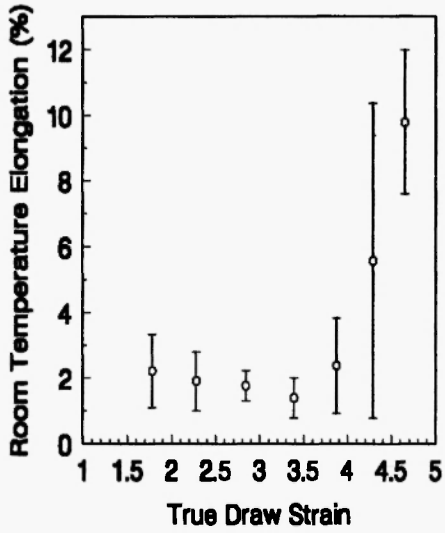

Figure 3: Room temperature tensile elongation vs. true draw strain. Tensile behavior changes from brittle to ductile at true strain between 3.4 and 3.8.

the room-temperature fracture behavior of tungsten wire changes from brittle to ductile at a true strain of between 3.4 and 3.8.

If we plot the tensile elongation data for 0.64 mm wire (the final drawing size) vs. average drawing temperature, we obtain a plot representing the effect of working history on wire ductility. This plot is shown for material swaged using schedule H (1300 C) in figure 4a and for material swaged using schedule L (1150 C) in figure 4b. These plots show that tensile elongation initially increases with average drawing

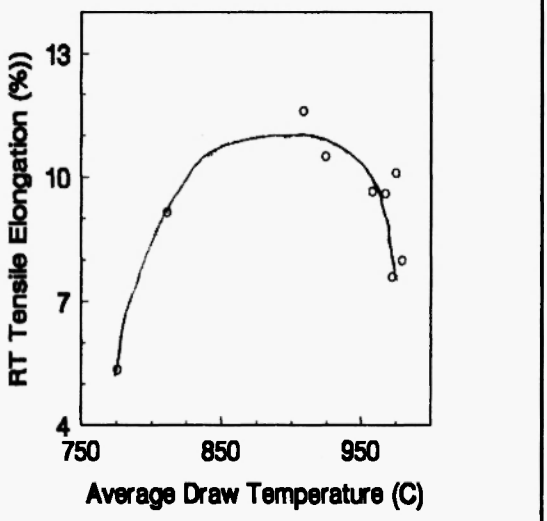

Figure 4a: Room temperature tensile elongation vs. average drawing temperature for samples swaged using swage schedule H. Ductility is maximized at intermediate average drawing temperatures.

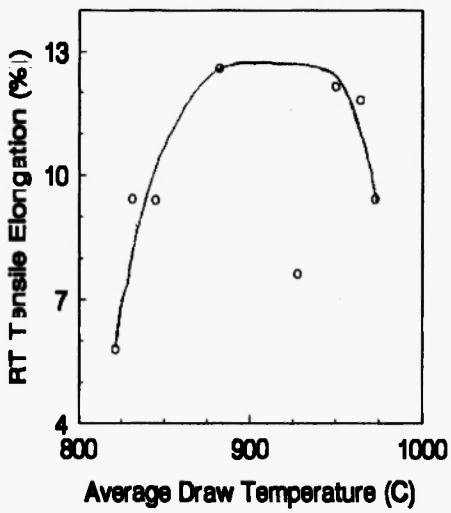

Figure 4b: Room temperature tensile elongation vs. average drawing temperature for samples swaged using swage schedule L. Ductility is maximized at intermediate drawing temperatures.

temperature, reaches a maximum at intermediate temperatures and then decreases once again at higher drawing temperatures. We also see that

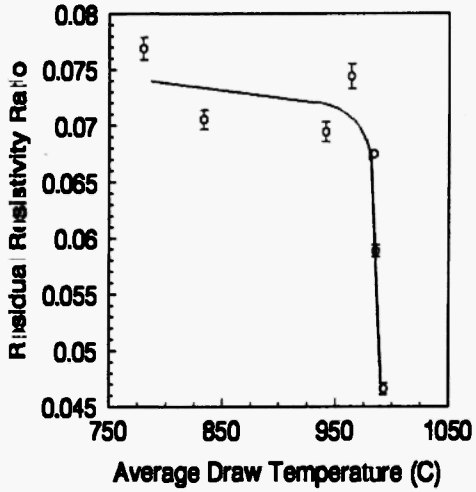

Figure 5: Electrical residual resistivity ratio as a function of average drawing temperature for 0.64 mm diameter wire. The ratio drops off at a temperature of approximately 975 C.

these two plots are very similar, although the 1150 C swage appears to result in higher elongation at intermediate drawing temperatures.

Residual resistivity ratio measurements were made at 0.64 mm diameter. The results are plotted as a function of average drawing temperature in figure 5. This figure shows the residual resistivity ratio dependence on working history of our samples. The residual resistivity ratio remained essentially constant at average drawing temperatures below approximately 975 C and then decreased significantly at higher average draw temperatures.

Figure 6 shows a TEM micrograph of the substructure of 3.40 mm diameter rod which was swaged at 1300 C (swage schedule H). The substructure is very polygonized, with the substructural cells having an aspect ratio of 1.93 ± 1.49. This would indicate that substantial dynamic polygonization had occurred at this swaging pass. One half of this rod was then drawn to 2.67 mm at 800 C, while the other half was drawn to 2.67 mm at 1100 C. Figures 7a and 7b show the substructures that resulted from these drawing temperatures. In the wire drawn at 800 C (figure 7a), the polygonized structure is still present, but the aspect ratio of substructural cells has increased to 3.12 ± 0.89. However, the aspect ratio of substructural cells in the wire drawn at 1100 C (figure 7b) is 1.07 ± 0.10, indicating that these are new cells that were formed through dynamic polygonization during drawing.

DISCUSSION:

In this section, we will attempt to rationalize our experimental results by discussing the role that dynamic recovery plays during wire drawing. For this reason, a brief review of the dynamic recovery of tungsten will be presented.

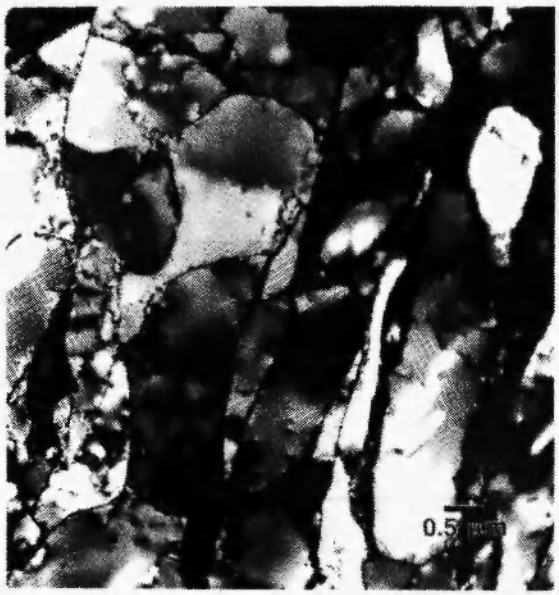

Figure 6: TEM photomicrograph showing a longitudinal cross-section of the substructure of 3.40 mm diameter swaged rod. The sample is polygonized, with subgrains having an aspect ratio of 1.93.

Figure 7a: TEM photomicrograph showing a longitudinal cross-section of the substructure of 2.67 mm diameter drawn wire which has been drawn at 800 C. Subgrains have an aspect ratio of 3.12 , indicating that polygonization did not occur during drawing.

Figure 7b: TEM photomicrograph showing a longitudinal cross-section of the substructure of 2.67 mm diameter drawn wire which has been drawn at 1100 C. Subgrains are equiaxed, having an aspect ratio of 1.07. This indicates that polygonization did occur during drawing.

A material containing a non-equilibrium distribution of defects will exhibit recovery if sufficient activation energy is supplied. This energy can be supplied in the form of thermal energy, stored energy (the energy of the defect structure itself) or externally applied mechanical energy[7]. When recovery is assisted by the mechanical energy of deformation and occurs in situ, this is termed dynamic recovery. The temperature required for recovery is lowered in this case. It is also lowered as the stored defect energy of a material is increased as it is mechanically worked to high strains[8].

Five stages of recovery have been identified in tungsten wire. The first and second of these stages were identified by Thompson[9]. They are concerned with very low temperature recovery and will not be of interest here. Schultz[10] and Welsch[11] investigated the final three stages of recovery in tungsten using electrical residual resistivity ratio measurements. Welsch postulated that stage three recovery involves the annihilation of point defects and oppositely signed dislocations as well as the rearrangement of self-interstitials. Burgers found evidence that activation energies are also high enough during this stage of recovery to allow for dislocation glide[12]. Welsch also found that residual resistivity ratio was relatively unaffected by this stage of recovery[11]. If enough energy is supplied to allow for dislocation climb, then dislocations can move out of their glide planes and align themselves with other dislocations to form low-angle grain boundaries within a fiber. These low-angle boundaries are called sub-boundaries, and this, the fourth stage of recovery in tungsten, is termed polygonization. Welsch and Hehemann found that a steep drop in residual resistivity ratio indicated the end of stage three dynamic recovery and the onset of polygonization[11]. The final stage of recovery involves grain or fiber growth and is associated with the onset of recrystallization.

The degree of recovery that is optimal during NS tungsten processing is not well understood. Because the stages of recovery discussed above have been associated with changes in the physical and mechanical properties of tungsten[13,14], we wished to make a quantitative determination of the effect that processing history would have on the metallurgical properties of tungsten wire. In particular, we were interested in developing methods that would allow for the accurate determination of the degree of dynamic recovery that would take place for a

given set of processing parameters and what the effect on wire ductility would be.

When recovery occurs, the physical and mechanical properties that suffered a change as a result of cold working tend to recover their original values[14]. In most metals, whose ductility decreases with increasing cold work, recovery causes an increase in ductility due to the recovery of strain hardening effects. In the case of tungsten, where ductility is increased with increasing deformation, one might expect that ductility would revert to lower values as a result of recovery. However, during stage three recovery the microstructure of tungsten is not changed and, because the ductility increase that occurs in tungsten with increasing deformation is directly related to microstructural development, we would expect that ductility would not decrease during this stage of recovery. In fact, we would expect the ductility of tungsten, like other metals, to increase during stage three recovery as a result of point defect annihilation. Dynamic recovery has also been shown to lead to a decrease in deformation flow stresses[13]. Therefore, during stage three recovery, we would expect to see an increase in room temperature tensile elongation and a decrease in deformation flow stresses.

In our samples, we found that room temperature tensile elongation was low for samples that were wire-drawn at very low temperatures but increased as the drawing temperature was increased to intermediate temperatures (figures 4a and 4b). In addition, we found that the low temperature slope change of the draw stress vs. draw temperature plot occurred at a different temperature for each wire size (figures 2a - 2c). This slope change would indicate that the flow stress of our samples was reduced. These two effects: increased ductility and decreased flow stress, would both be consistent with the onset of stage three dynamic recovery. A plot of the temperatures at which these phenomena occurred in our samples as a function of true strain is shown in figure 8. It should be noted that the ductility increase temperature was not discernible for three of the seven drawing passes investigated (2.67 mm, 1.19 mm and 0.94 mm). A possible explanation for the lack of a discernible ductility increase temperature at 2.67 mm, which is the first drawing pass, is that wire ductility would be more dependent on the swaging history than on the drawing history since only one drawing pass had occurred. The data from the 1.19 mm and 0.94 mm diameter wire sizes was difficult to interpret

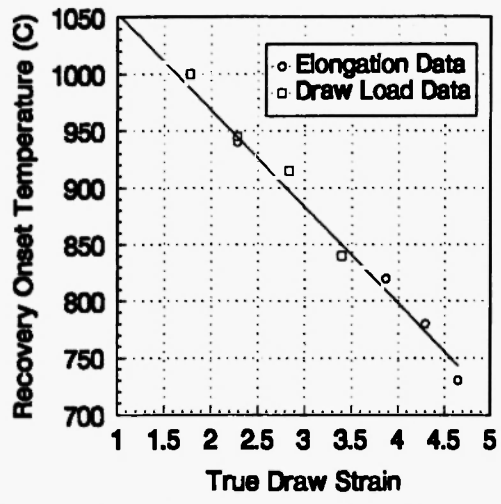

Figure 8: Onset temperature of RT elongation increase and draw stress reduction vs. true draw strain. Wire drawn at temperatures below this line for a given draw pass had reduced ductility..

because at these wire sizes the DBTT of NS tungsten is very close to room temperature, which caused large variations in room temperature tensile results. However figures 2a, 2b and 2c show that slope changes in the draw force vs. draw temperature plots were clearly evident at these wire sizes and were consistent with the expected results. Notice that the relationship is linear and that the temperatures of ductility increase and draw force slope change lie on the same line (within experimental error). Our experimental results therefore suggest that figure 8 represents the onset drawing temperature of stage three dynamic recovery as a function of true strain. Or, more precisely, the plot indicates the temperature, for a range of wire diameters, at which dynamic recovery begins to have a measurable effect on flow stress and room temperature ductility.

We also found that RT tensile elongation decreased as the average drawing temperature was increased from intermediate to high values (figures 4a and 4b) and that samples drawn with high average drawing temperatures had much lower residual resistivity ratios than samples that had been drawn at low and intermediate temperatures (figure 5). Meiren et al found in static annealing experiments that polygonization caused a decrease in the ductility of NS tungsten because of the increase in transverse grain boundary density that results[15]. Welsch has shown that a sharp decrease in the residual resistivity ratio of tungsten indicates the transition from stage three recovery to polygonization[6]. If the ductility decrease temperatures are plotted vs. true strain, we obtain the plot shown in figure 9. Our experimental results would therefore suggest that figure 9 represents the onset temperature of dynamic polygonization. As was the case in figure 8, the relationship is linear. Notice that the polygonization onset temperature for 2.67 mils diameter (true strain = 1.78) shown in

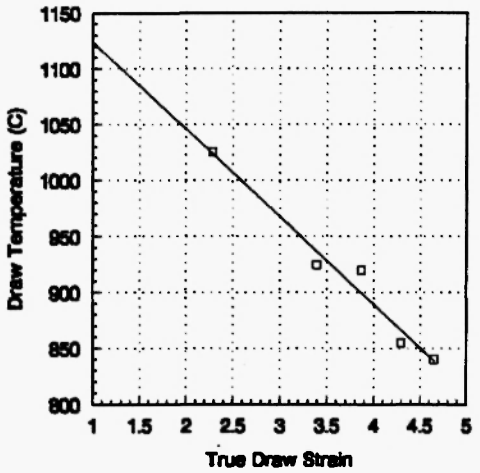

Figure 9: Temperature of RT elongation decrease vs. true draw strain. Wire drawn at temperatures above this line at a given drawing pass had reduced tensile elongation at room temperature.

figure 9 is approximately 1065 C. This would explain why TEM analysis indicated that polygonization had occurred in a sample that had been drawn to this diameter at a temperature of 1100 C (figure 7b).

The information represented in figures 8 and 9 can be used to predict the microstructural state and mechanical properties that would result from a given thermomechanical history. However, the limitations of this work should be considered.

First, it is important to realize that these plots represent the state of dynamic recovery that has resulted from a wire's entire thermomechanical processing history and must be interpreted as such. They are meant to be used as a tool for forecasting the effect of an integrated working history - not for individual drawing passes. Furthermore, drawing temperatures are assumed to decrease in an approximately linearly fashion with increasing true strain. Substantial deviations from this assumption may yield contradictory results.

CONCLUSIONS:

We have developed a method for quantifying the effect of thermomechanical processing history on microstructural and mechanical wire properties. This study has allowed us to develop the understanding required to make quantitative determinations of how tungsten wire will respond to a given thermomechanical processing history. Material properties have been found to be dependent on the degree of dynamic recovery that has taken place during wire drawing. The degree of dynamic recovery that tungsten wire will undergo has been found to be a function of the wire drawing temperature and the true drawing strain (which is a function of the wire diameter). If dynamic recovery does not occur, tungsten wire will have low ductility. If dynamic recovery occurs without

polygonization, then tungsten wire will have maximum ductility. If drawing temperatures are high enough to cause dynamic polygonization to occur, then tungsten's ductility will be decreased. We can therefore conclude that a thermomechanical processing history which produces dynamic recovery without causing dynamic polygonization will maximize wire ductility.

Perhaps the most important conclusion from this work is that the properties of tungsten wire are *history dependent*. It is very difficult to make any sort of judgment as to the effect of a process change at any given part of the process without simultaneously considering the overall working history.

References:

1. Yih, W.H.T. and Chun, T.W., eds.: Tungsten: Sources, Metallurgy, Properties and Applications, Plenum Press, New York (1979). pp. 276.
2. Yih, W.H.T. and Chun, T.W., eds.: Tungsten: Sources, Metallurgy, Properties and Applications, Plenum Press, New York (1979). pp. 271.
3. Coolidge, W.T.: US Patent 1082993.
4. Peck, J.F. and Thomas, D.A.: *Met Trans* 221, (1961) pp. 1240 - 1246
5. Hennessy, D.R., General Electric Tungsten Products Plant, Personal Communication
6. Welsch, G.E., Young, B.J., Hehemann, R.F.: Proceedings of the 5th International Conference of the Strength of Metals and Alloys, (1979)
7.. Bever. M.B.: Creep and Recovery, American Society for Metals, Cleveland, OH. (1956) pp. 46
8. Bever. M.B.: Creep and Recovery, American Society for Metals, Cleveland, OH. (1956) pp. 23
9. Thompson, M.W.: Defects and Radiation Damage in Metals, Cambridge University Press. (1969) pp. 301-304.
10. Schultz, H.: *Acta Met* 12, (1964) pp. 649-664.
11. Welsch, G.E. and Hehemann, R.F.: General Electric Report 78-LRL-1628 (1978), General Electric Lighting Research Laboratory Library, Nela Park, Cleveland, OH
12. Burgers, W.G.: Strength of Solids: Report of 1947 Conference, Physical Society. (1947) pp. 134.
13. Dieter, G.E.: Mechanical Metallurgy, 3rd Edition, McGraw-Hill Book Company, New York, NY. (1986) pp. 534-535.
14. Reed-Hill, R.E.: Physical Metallurgy Principles, Van Nostrand Reinhold Company, New York, NY. (1964) pp. 179.
15. Meiren, E.S. and Thomas, D.A.: *Met Trans* 233, (1965), pp. 937 - 943.